set of possible, *received* signal values, after interaction with the noise. The amount of information H_T actually conveyed by the definite decision "yes," or "no," is given by the well-known[2] expression

$$H_T = H(\mathbf{x}) - H(\mathbf{y}|\mathbf{x}), \tag{1}$$

where $H(\mathbf{x})$ is the information content of the original, input $\mathbf{x}$, and $H(\mathbf{y}|\mathbf{x})$ is the conditional entropy, or uncertainty in $\mathbf{x}$ based on knowledge of the received wave $\mathbf{y}$, i.e., the *equivocation*. If p and q are, respectively, the *a priori* probabilities of signal and no-signal, e.g., $p+q=1$, it is clear that

$$H(\mathbf{x}) = -p\log p - q\log q, \quad (\ )/\text{indication}, \tag{2}$$

the units of information being (bits/indication or decision) if 2 is chosen as the base of the logarithm, in the usual way. (For $p=q=\frac{1}{2}$, $H_{\max}(\mathbf{x})=1$ bit/indication.)

The equivocation may be calculated as follows: let x_1 be a value of x associated with a signal; x_2, with no signal; and y_1, a value of the received wave, associated with a "yes" decision; y_2 is associated with a "no" decision. The probabilities of the various possibilities indicated above then are, if we remember that there are two types of error that can occur in any decision,

$$\begin{aligned} &P(x_1, y_1) = p(1-\beta); \quad P(x_1, y_2) = p\beta; \\ &P(x_2, y_1) = q\alpha; \qquad\quad P(x_2, y_2) = q(1-\alpha), \end{aligned} \tag{3}$$

and the equivocation is

$$H(\mathbf{y}|\mathbf{x}) = -\sum_{k,j=1}^{2} P(x_j, y_k)\log\left[\frac{P(x_j, y_k)}{P(y_k)}\right]. \tag{4}$$

The marginal probabilities needed here are: $P(y_1)=p(1-\beta)+q\alpha$; $P(y_2)=p\beta+q(1-\alpha)$. The equivocation becomes explicitly

$$\begin{aligned} H(\mathbf{y}|\mathbf{x}) = H(\mathbf{x}) - [&p(1-\beta)\log\{(1-\beta)/[p(1-\beta)+q\alpha]\} \\ &+p\beta\log\{\beta/[p\beta+q(1-\alpha)]\}+q\alpha\log\{\alpha/[p(1-\beta)+q\alpha]\} \\ &+q(1-\alpha)\log\{(1-\alpha)/[p\beta+q(1-\alpha)]\}]. \end{aligned} \tag{5}$$

One easily shows that the equivocation is a *maximum* when $\alpha+\beta=1$, and in fact is equal to $H(x)$, which is not unreasonable, as with completely wrong decisions no information remains upon detection, i.e., $H_T=0$, Eq. (1). One does better to guess on the basis of the *a priori* probabilities. At the other extreme, if $\alpha=\beta=0$, $H_T=H(\mathbf{x})$; as expected, no information is lost, since there is no error in decision.

Two cases of particular interest arise: (a) when α is very small, in the radar problem (small false-alarm times), and (b) when $\alpha=\beta$, in the many situations where there is no reason to weight errors of the second kind more heavily than the first.[3] We have

$$(\alpha\doteq 0;\ \beta>0):\ H(\mathbf{y}|\mathbf{x}) \doteq -q\log q - p\beta\log p\beta + (p\beta+q)\log(p\beta+q), \tag{6}$$

$$(\alpha=\beta):\ H(\mathbf{y}|\mathbf{x}) = H(\mathbf{x}) - (1-\alpha)\log(1-\alpha) - \alpha\log\alpha + \sum_{k=1}^{2} P(y_k)\log P(y_k). \tag{7}$$

As an example, let us compare the Neyman-Pearson and Ideal observers[1] in two instances, assuming equal *a priori* probabilities in both cases, and equal input signal-to-noise ratios (i.e., the constraints on the channel for both observers are the same). The probabilities of Type I and Type II errors are, of course, different in general. From the data of Figs. 4 and 5 of reference 1 (Paper II), and with the help of (6) and (7), (1) and (2), we may tabulate the important quantities, remembering [see (2)] that $H(\mathbf{x})=1$ bit/indication when $p=q=\frac{1}{2}$.

The Ideal observer, for the same input signal-to-noise ratio (a_0^2), and integration time ($\sim n$), is seen to be better than the Neyman-Pearson observer in the same circumstances: less information is lost when the decision is made (larger H_T) and this in turn is reflected in the smaller probability of an incorrect decision $(\alpha+\beta)/2$, $p=q=\frac{1}{2}$ [from the unnormalized betting curves, see Sec. (4)–(6) of reference 1]. [For normalized betting curves, $\alpha+\beta$ represents the total probability of an incorrect decision here ($p=q=\frac{1}{2}$).] That the Ideal observer is better than the Neyman-Pearson is consistent with the definition of the former as minimizing the total probability of wrong decisions (for the same integration time and input ratio a_0^2).[1,4] Another comparison, on the basis of *equal* probabilities of error, confirms the superiority of the Ideal observer from the point of view of signal threshold. From the second and third rows of Table I, we find that the Neyman-Pearson observer loses less information in decision by 0.043 bit/indication than does the Ideal, but requires at the same time a threshold signal (if the noise background and integration time are held constant) 2.0 db [$=10\log_{10}(5.0/3.15)$] stronger. Finally, we note that the Sequential observer,[1] for the same values of α, β chosen for the Ideal or the Neyman-Pearson cases, yields the same equivocations as indicated above, see Table I and (5), with the same comparisons on that score, but always on the average for *smaller* ratios of $a_0^2\langle n\rangle^{\frac{1}{2}}$. Thus, for the same input ratios $a_0^2\sqrt{n}=a_0^2\langle n\rangle^{\frac{1}{2}}$, α and β, and hence $H(\mathbf{y}|\mathbf{x})$ will be correspondingly smaller. A detailed study of the interdependence of threshold, integration time, α and β, and information loss is being prepared.[5]

TABLE I.

Observer	Threshold constant (weak signal)	α	β	Total prob. of error $(\alpha+\beta)/2$	$H(\mathbf{y}\|\mathbf{x})$	H_T
Neyman-Pearson	$a_0^2\sqrt{n}=3.15$	10^{-4}	0.73	0.365	0.850 bit	0.150 bit
Ideal	3.15	0.05	0.05	0.05	0.285	0.715
Neyman-Pearson	$a_0^2\sqrt{n}=5.0$	10^{-4}	0.10	0.05	0.242	0.758
Ideal	5.0	0.01	0.01	0.01	0.080	0.920

* The research reported here was done by the author as a consultant to the Lincoln Laboratory, The Massachusetts Institute of Technology (Cambridge, Massachusetts), and is published by permission, which is gratefully acknowledged. The research in this document was supported jointly by the U. S. Army, Navy, and Air Force under contract with the Massachusetts Institute of Technology.

† Consultant, Lincoln Laboratory, Massachusetts Institute of Technology.

[1] D. Middleton, J. Appl. Phys. **24**, 371, 379 (1953); also "Statistical methods for the detection of pulsed radar in noise," proceedings of a symposium (London, September, 1952) on *Applications of Communication Theory* (Academic Press, Inc., New York, 1953).

[2] C. E. Shannon, Bell System Tech. J. **27**, 379, 623 (1948).

[3] Reference 1 and D. Middleton, J. Appl. Phys. (Letter to the Editor, to be published).

[4] D. Middleton, Letter to the Editor, J. Appl. Phys. (to be published).

[5] D. Middleton, "The Statistical Theory of Detection, III; Entropy Changes and Information Loss," a Lincoln Laboratory report.

Discussion of "Statistical Criteria for the Detection of Pulsed Carriers in Noise I, II"

D. MIDDLETON, *Cruft Laboratory, Harvard University, Cambridge, Massachusetts*

AND

W. W. PETERSON AND T. G. BIRDSALL, *Engineering Research Institute, University of Michigan, Ann Arbor, Michigan*

(Received September 12, 1953)

THESE papers[1] represent the first unified presentation of the application of several types of statistical tests to the important problem of detection in communication theory. However, we feel that the comparison of tests considered in paper II is of somewhat limited scope and that a clearer and more complete account of the author's methods of comparison is needed.

A comparison of statistical observers may be made in a number of ways: in fact, we observe first that in many situations there is no necessity for comparing the Neyman-Pearson, Ideal, and Sequential observers[2]—each is an optimum procedure for the problem at hand.[3,4] However, our choice of observers in some instances may be based on which is the best *for a given total*

probability $(\alpha q+\beta p)$ *of decision error*. Then the comparisons discussed at length in paper II, reference 1, follow. (We recall that α and β are, respectively, the probabilities of a Type I and a Type II error, and that p and q are the *a priori* probabilities associated with signal plus noise, and noise alone.[2])

Two possibilities exist under this condition: (1) the comparison is made on the basis of the unnormalized betting curves W; (2) the comparison is given in terms of *normalized* betting curves,[5] with the best observer defined in each instance as the one giving the largest value of the betting curve for a given threshold (a_0^2)

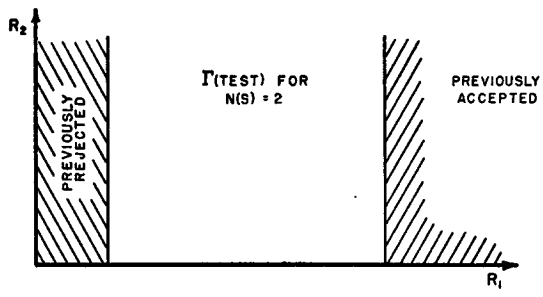

FIG. 1.

and observations time (n) (or equivalently, the same value on the betting curve for the smallest threshold). Paper II considered case (2) only and did not emphasize the normalized character of the betting curves under comparison. Accordingly, we include a short table (Table I), comparing the Neyman-Pearson and Ideal observers, subject to the same value of the sum $\alpha q+\beta p$. (The equal signs mean "equally good;" $\gtrless$ indicate "better than" or "worse than," and p, q, n are held fixed for any particular comparison.)

The tests are identical (for fixed a_0, n, p, q) when $\alpha_{NP}=\alpha_{I(\min)}$, and thus $\beta_{NP(\min)}=\beta_{I(\min)}$, and $K=1$, [see Eqs. (4.5) and (4.6), reference 1]. When the tests are not identical, $\alpha_{NP}\neq\alpha_{I(\min)}$, etc., then *by definition* the Ideal observer is best, in the sense of the *unnormalized* comparison, since he minimizes the total probability of decision error, while the Neyman-Pearson observer has α_{NP} already fixed, and can only minimize β. On the basis of normalized betting curves, however, the Neyman-Pearson observer is sometimes better than the Ideal. This is the result of the normalization procedure. This explains why the former gives a smaller minimum detectable signal than the latter (same $\alpha q+\beta p$), as shown in Fig. 7, $\alpha=0.05$ (reference 1), and why in Fig. 8, $\alpha=0.05$, the reverse

TABLE I.

	Conditions	Unnormalized	Normalized
I	$\alpha p \doteq 0$	$NP=$Ideal	$NP\doteq$Ideal
$\alpha_{NP}=\alpha_I$; $\beta_{NP}=\beta_I$ (Identical tests)	$\alpha(p-q)\doteq 0$ other αp, $\alpha(p-q)$	$NP=$Ideal	$NP>$Ideal
II $W_{NP}<W_I<\frac{W_{NP}-\alpha_{NP}(2q-p)}{1-\alpha_{NP}}$ $(q<p)$ (Nearly-identical tests)		$NP<$Ideal	$NP>$Ideal
III $\alpha_{NP}\neq\alpha_{I(\min)}$; $\beta_{NP}\neq\beta_{I(\min)}$ (and not II) (Non-identical tests)		$NP<$Ideal	$NP<$Ideal

situation appears. (For a brief mention, see reference 4.) The normalization also accounts for the apparently greater amount of information following the decisions operation for the Neyman-Pearson observer, as shown in the comparison of lines 2 and 3 (Table I), in a recent "Letter to the Editor."[6] We remark, finally, that the Sequential observer, for the same α, β, p, q, will yield a lower threshold for the same average integration time, or equivalently, for the same threshold, a shorter average observation period, than either the Neyman-Pearson or the Ideal observers.

The indicated calculation of the betting curves in reference 1 for the Sequential observer, Eqs. (6.2), (6.5), is not correct, although Eq. (6.1) is valid, provided we determine P_n and Q_n properly. Unfortunately, we cannot find P_n and Q_n as was done for the fixed sample tests (Neyman-Pearson, etc.), in as much as the Sequential observer deals at any stage n (before a decision is reached at $n=n(s)$) *only* with those signals which have not been previously accepted or rejected. The remaining signals will yield distributions of the logarithm of the likelihood ratio (the P_n, Q_n) quite different from the distributions derived on the basis of all possible signals, on which the calculations [Eq. (4.12)] for the Neyman-Pearson and Ideal observers are based. Thus, instead of (4.3) or (4.12) we have for the distributions of the logarithm (x) of the likelihood ratio, expressions of the type

$$P_{n(s)}(x;a_0)=c_{n(s)}\int_{\Gamma(\text{test})}\cdots\int W_{n(s)}(R_1\cdots R_{n(s)}|a_0)dR_1\cdots dR_{n(s)}\delta(x-\log\Lambda_{n(s)}), \quad (1)$$

$$Q_{n(s)}(x;a_0)=d_{n(s)}\int_{\Gamma(\text{test})}\cdots\int W_{n(s)}(R_1\cdots R_{n(s)}|0)dR_1\cdots dR_{n(s)}\delta(x-\log\Lambda_{n(s)}), \quad (2)$$

where $c_{n(s)}$ and $d_{n(s)}$ are constants such that

$$\int_{-\infty}^{\infty}P_{n(s)}(x;a_0)dx=1=\int_{-\infty}^{\infty}Q_{n(s)}(x;a_0)dx, \quad (3)$$

and the test region $\Gamma(\text{test})$ consists of all envelopes $(R_1\cdots R_n\cdots \times R_{n(s)})$ such that

$$\frac{\beta}{1-\alpha}\leq\Lambda_n(R_1\cdots R_n)\leq\frac{1-\beta}{\alpha} \text{ for all } n<n(s). \quad (4)$$

This makes the explicit evaluation of P and Q technically quite complicated. For example, in the very simple case where $\log\Lambda_{n(s)}$ is proportional to the sum of the squares of the envelope samples,

$$\log\Lambda_n=g(n)\sum_1^n R_i^2, \quad (5)$$

for $n(s)=2$ the test region $\Gamma(\text{test})$ is all (R_1, R_2) that satisfy condition (4), namely,

$$\log\frac{\beta}{1-\alpha}\leq g(1)R_1^2\leq\log\frac{(1-\beta)}{\alpha}, \quad (6)$$

and is shown graphically in Fig. 1. For $n(s)=3$, the test region is all (R_1, R_2, R_3), satisfying both Eqs. (6) and (7),

$$\log\frac{(1-\alpha)}{\beta}\leq g(2)[R_1^2+R_2^2]\leq\log\frac{(1-\beta)}{\alpha}. \quad (7)$$

The reason for this is that at the second stage those (R_1, R_2) in the test region that satisfy

$$g(2)[R_1^2+R_2^2]>\log\frac{1-\beta}{\alpha} \quad (8)$$

are accepted, and those in the test region that satisfy

$$g(2)[R_1^2+R_2^2]<\log\frac{\beta}{1-\alpha} \quad (9)$$

are rejected (leading to the conclusion that only noise was present). Therefore, the test region for the next (3rd) stage is all those (R_1, R_2, R_3) that satisfy (7) but not either (8) or (9), and is the infinite cylinder with base as in Fig. 2. Clearly the test region becomes more complex at each step, and it appears to be a very difficult task to describe the test region and calculate the integrals (1) and (2) for all values of $n(s)$.

When (1) and (2) have been found, Eq. (6.3) may then be used to obtain the mean betting curve, which results when we average over all possible $n(s)$ for which the test just terminates. The discrepancy between the calculations for the Sequential observer

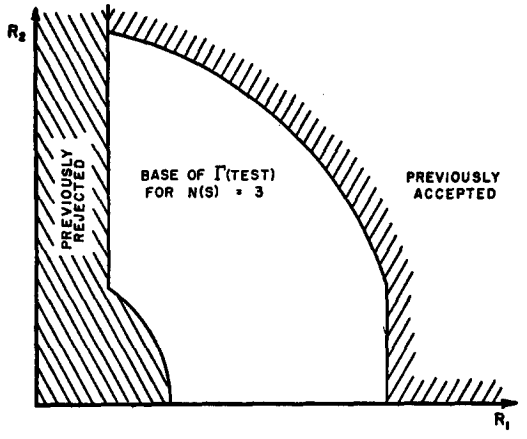

FIG. 2.

shown in Figs. 8 and 9 and the expected superiority of this observer over the others for the same controls is explained primarily in terms of the foregoing error, The necessarily crude approximations to the distribution of sample size, as originally indicated in paper II, also plays a part in this discrepancy.

[1] D. Middleton, J. Appl. Phys. 24, 371 (I), 379 (II) (1953). Also, a condensed account of this work appears in *Applications of Communications Theory*, edited by Willis Jackson (Academic Press, New York, 1953).
[2] For a description, see reference 1, paper I.
[3] W. W. Peterson and T. G. Birdsall, "The theory of signal detectability," Technical Report No. 13, Electronic Defense Group, Engineering Research Institute, Department of Electrical Engineering, University of Michigan, discuss in detail the Neyman-Pearson and Ideal observers on this basis.
[4] D. Middleton, J. Appl. Phys., 24, 127(L) (1953), also mentions some specific applications where the type of observer is specified beforehand by the problem in question.
[5] The specific normalizations are indicated in Eqs. (7.7a-c), reference 1.
[6] D. Middleton, "Information loss attending the decision operation in detection" J. Appl. Phys. 24, 127(L) (1953).

A Method for Generating Strong Shock Waves

A. HERTZBERG AND W. E. SMITH
Cornell Aeronautical Laboratory, Inc., Buffalo, New York
(Received September 30, 1953)

EXPERIMENTAL research into the physical phenomena associated with hypersonic flow[1] and high-temperature gas dynamics[2] is characterized by its dependence currently upon successful generation of shock waves whose strengths correspond to Mach numbers greater than ten. To this end, attention has been directed toward development of suitable techniques involving either explosive charges,[3] electrical discharge tubes,[4] or especially high-pressure-ratio shock tubes.[5] The shock tube excels in its simplicity and versatility. The present note is to discuss a simple modification of the operation of the combustion-powered, high-pressure-ratio shock tube which permits extension of its range.

The tendency has been to employ as driver a gas, or gases, whose temperature is high and whose molecular weight is low, so that the corresponding acoustic velocity is maximized. The influence of the acoustic velocity in the driver gas is illustrated in Fig. 1, where the diaphragm pressure ratio required to produce a certain shock strength is given for various speed-of-sound ratios. A simple method for obtaining a high acoustic velocity in the driver is by burning a combustible gaseous mixture in the driver chamber at constant volume. Unfortunately, the maximum temperature to which the driver can be heated is limited by the onset of molecular dissociation. Its molecular weight is likewise limited by practical combustion mixtures. In general, it is not feasible to operate a shock tube in which the speed-of-sound ratio exceeds 6.6 (approximately). Thus, the shaded area in Fig. 1 is unavailable to the experimenter employing a constant-volume combustion cycle.

To drive a shock wave through air, a stoichiometric mixture of oxygen and hydrogen diluted with 80 percent helium has been adopted at Cornell Aeronautical Laboratory. Shock Mach number of about 17 with a pressure ratio of 17 200 may be obtained from this mixture. To maintain appreciable densities in the low-pressure chamber, however, high pressures in the driver chamber are required. To accommodate a significant volume within a large-bore shock tube, then, the structural problems become prohibitive. Methods for obtaining effectively higher driver speeds must be developed if the application of the shock tube in the Mach-number range above ten is not to be severely limited.

In the course of hypersonic-flow investigations with the combustion-powered shock-tube facility at Cornell Aeronautical Laboratory, it has been discovered that higher shock speeds than can be explained by the theory of constant-volume burning are obtained under certain conditions. The anomalous results, although at first dismissed as being due to experimental error arising from the instrumentation, were eventually shown to be unexplainable by any orthodox analyses. Furthermore, in every case, the unexpected "efficiency" was correlated with the application of diaphragms (separating high- and low-pressure regions) which were accidentally weaker than those designed to withstand complete combustion at constant volume. As a consequence, a subsidiary investigation was launched. Diaphragms of varying thickness to withstand pressures corresponding to the full range of possible completion of combustion (from none to fully complete) were tested while holding fixed the initial (pre-ignition) pressures of the driver and driven gases. The test results are shown in Fig. 2.

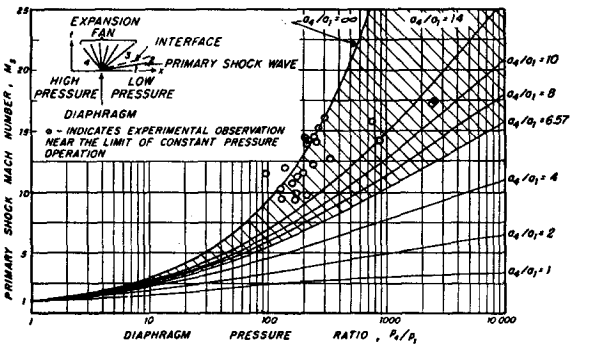

FIG. 1. Shock-tube performance curves and test data. p_1, p_4 are total pressures acting on the diaphragm at instant of failure. a_1, a_4 are sound velocities in the high and low pressure regions after combustion at constant volume is completed and before the diaphragm bursts. The adiabatic exponents, γ_1 and γ_4, are each taken to be 1.40. Because of the limitation on a_4, the shaded region is inaccessible for constant volume operation.

The excessive scatter arises largely from practical difficulties involved in determining the shock Mach number, for the shock front may consist of multiple shock waves for several tube diameters downstream of the diaphragm.

It is seen that the shock Mach number varies *inversely* as the measured bursting pressure of the diaphragm. Thus, the highest shock strength is realized when the diaphragm is destroyed immediately after ignition. In this case, the combustion proceeds within the driver gases as they issue forth at constant pressure into the low-pressure chamber. Should the diaphragm fail after combustion is partially completed, the shock strength is intermediate between the limits represented by constant pressure and constant volume cycles. Multiple shock fronts are characteristic phenomena of these "in-between" cycles. It has been demonstrated by carefully recording and analyzing the pressure history within the burning gases that detonation phenomena are absent from the combustion processes here described. Preliminary data on operation near the constant-pressure limit are shown in Fig. 1 and indicate the extent to which the shaded area becomes accessible. It appears that for a given diaphragm pressure ratio the "constant pressure" process permits attainment of the limiting